

Freeze and Conquer: Reusable Ansatz for Solving the Traveling Salesman Problem

Fabrizio Fagiolo^{1,*} Nicolò Vescera^{2,*}

¹ National Research Council (CNR), Rome, Italy

² Università degli Studi di Perugia, Perugia, Italy

fabrizio.fagiolo@istc.cnr.it nicolo.vescera@collaboratori.unipg.it

Abstract

In this paper we present a variational algorithm for the Traveling Salesman Problem (TSP) that combines (i) a compact encoding of permutations, which reduces the qubit requirement too, (ii) an optimize-freeze-reuse strategy: where the circuit topology (“Ansatz”) is first optimized on a training instance by Simulated Annealing (SA), then “frozen” and re-used on novel instances, limited to a rapid re-optimization of only the circuit parameters. This pipeline eliminates costly structural research in testing, making the procedure immediately implementable on NISQ hardware.

On a set of 40 randomly generated symmetric instances that span 4 – 7 cities, the resulting Ansatz achieves an average optimal trip sampling probability of 100% for 4 city cases, 90% for 5 city cases and 80% for 6 city cases. With 7 cities the success rate drops markedly to an average of $\sim 20\%$, revealing the onset of scalability limitations of the proposed method.

The results show robust generalization ability for moderate problem sizes and indicate how freezing the Ansatz can dramatically reduce time-to-solution without degrading solution quality. The paper also discusses scalability limitations, the impact of “warm-start” initialization of parameters, and prospects for extension to more complex problems, such as Vehicle Routing and Job-Shop Scheduling.

1 Introduction

Solving combinatorial optimization problems is among the most prominent applications of quantum computing. Two main paradigms have emerged to tackle such problems: quantum annealers, which are specialized hardware devices designed to minimize a cost Hamiltonian, and gate-based quantum processors, which implement Variational Quantum Algorithms (VQAs) such as the Variational Quantum Eigensolver (VQE) and the Quantum Approximate Optimization Algorithm (QAOA). However, when dealing with NP-hard combinatorial problems such as the Traveling Salesman Problem (TSP), two recurring bottlenecks emerge in quantum technology: (i) the use of $\mathcal{O}(n^2)$ qubits in standard QUBO/HUBO encodings, which require heavy penalty terms to enforce feasibility, and (ii) deep, fixed circuit layouts that are ill-suited to the constraints of NISQ devices.

In this work, we use the Variational Quantum Eigensolver (VQE), where one prepares a parameterized Ansatz \mathcal{A} , $|\psi(\boldsymbol{\theta})\rangle$, and adjusts the parameter vector $\boldsymbol{\theta}$ so as to minimize

$$E(\boldsymbol{\theta}) = \langle \psi(\boldsymbol{\theta}) | \hat{H} | \psi(\boldsymbol{\theta}) \rangle,$$

thereby obtaining an approximation of the ground-state energy E_{\min} of \hat{H} [1, 2]. The shallow depth and flexibility of the circuit make VQE particularly suitable for NISQ hardware [4, 5].

*These authors contributed equally.

Another approach to solving the combinatorial optimization problem is the Quantum Approximate Optimization Algorithm (QAOA) that alternates p layers of two unitaries,

$$U_C(\gamma_k) = e^{-i\gamma_k \hat{H}_C}, \quad k = 1, \dots, p, \quad \hat{H}_B = \sum_{j=1}^n X_j,$$

$$U_B(\beta_k) = e^{-i\beta_k \hat{H}_B},$$

to construct the variational state.

$$|\psi_p(\boldsymbol{\gamma}, \boldsymbol{\beta})\rangle = \left(\prod_{k=1}^p U_B(\beta_k) U_C(\gamma_k) \right) |+\rangle^{\otimes n},$$

where $\boldsymbol{\gamma} = (\gamma_1, \dots, \gamma_p)$ and $\boldsymbol{\beta} = (\beta_1, \dots, \beta_p)$ are optimized to minimize $\langle \hat{H}_C \rangle$ [6, 7]. Because the circuit explicitly mirrors \hat{H}_C , the exploration of the Hilbert space is biased toward states that are relevant to the target optimization problem.

The Traveling Salesman Problem serves as our case study in this work. Let $V = \{v_1, \dots, v_n\}$ be a set of n cities and let $c : V \times V \rightarrow \mathbb{R}_{\geq 0}$ be a non-negative cost function with $c_{ij} = c(v_i, v_j)$. A *tour* is a permutation $\pi \in S_n$ of $\{1, \dots, n\}$ that induces the closed walk $v_{\pi(1)} \rightarrow v_{\pi(2)} \rightarrow \dots \rightarrow v_{\pi(n)} \rightarrow v_{\pi(1)}$ with total cost

$$C(\pi) = \sum_{k=1}^n c_{\pi(k), \pi(k+1)}, \quad \text{with the convention } \pi(n+1) = \pi(1).$$

The optimization task is to find $\pi^* \in S_n$ by minimizing $C(\pi)$ over all $n!$ permutations. Computing π^* is NP-hard and exact methods quickly become impractical as n grows.

In the VQE/QAOA formulations of the TSP, one of the first fundamental design choices concerns the encoding of permutations in qubits. Instead of QUBO/HUBO encodings, we adopt compact representations such as Lehmer encoding or permutation encoding [8] that reduce the number of qubits needed to $\mathcal{O}(n \log n)$. From this encoding, we develop a two-step workflow inspired by Machine Learning (ML) methods. During the training phase, a Simulated Annealing (SA) procedure jointly explores and learns the circuit topology and its parameters. In the subsequent test phase, the learned topology is frozen and the parameters are only slightly re-optimized, allowing a direct evaluation of the generalization ability.

Rather than deriving a Hamiltonian of the TSP in closed form, we estimate the objective value by sampling: at each measurement, we translate the outcome into a tour, compute its classical cost, and use the average cost as an estimate of the expected energy; instead, the solution is the minimum cost tour among those generated by the circuit. This allows us to perform variational optimization without explicitly writing the Hamiltonian.

The remainder of the paper is organized as follows. Section 2 describes the related work. Section 3 introduces the scheme of the proposed approach. Section 4 describes and comments on the experimental results. Section 5 ends the paper by providing some concluding remarks as well as possible future research lines.

2 Related work

In the Variational Quantum Algorithm (VQA), \mathcal{A} defines the set of states reachable by the circuit, effectively delimiting the space of explorable solutions. In the chemical-quantum domain, for example, it has already been shown that the choice of \mathcal{A} from the hardware efficient circuits of Kandala et al.[2] decisively affects the trade-off between circuit depth and accuracy of results.

The same is true for combinatorial problems such as TSP. Venkat et al. [13] show that both the architecture (annealer versus gate-based) and the shape of \mathcal{A} decisively affect solution quality and computation time. Murhaf et al.[14], exploiting D-Wave’s Pegasus topology and a QUBO reformulation that eliminates the initial node, achieve better tours than D-Wave’s “standard” TSP solver and arrive at 20 cities with fewer qubits. In contrast, the unoptimized approach of Jain et al.[15] stops at 8 cities without showing competitive performance.

Despite the limited number of qubits, gate-based computers can still hold their own against annealers through targeted encoding and \mathcal{A} . Ruan et al.[16] integrate TSP constraints into the QAOA

mixer, halve the qubits needed and double the probability of finding the optimal tour. Qian et al.[17] test three alternative mixers, improved edge-based coding and layered learning, achieving the best trade-off between depth and quality even in the presence of realistic noise.

Finally, Meng Shi et al.[18] propose APIs that automatically transform any problem on graphs (including TSP) into circuits solved by VQA, achieving with not too many qubits solutions equal to or better than those of specialized algorithms.

The most recent literature points out that, in VQA, it is not only the shape of \mathcal{A} that determines performance, but also how parameters are initialized and updated.

Egger et al.[25] introduce the warm-starting quantum optimization paradigm, showing that the choice of initial parameters obtained from a classical relaxation accelerates convergence without compromising quality guarantees. In a complementary study, Montañez-Barrera et al.[26] show that parameters optimized on small instances of QAOA can be successfully transferred to larger instances, and even to other combinatorial problems, while maintaining high accuracy of the solutions. Similarly, with Meta-VQE, Cervera-Lierta et al.[27] train a one time set of parameters that quickly adapts to different Hamiltonian configurations, reducing optimization time by orders of magnitude.

Moving in this direction, we propose a freeze & reuse strategy for the TSP: we design a compact \mathcal{A} that is capable of finding good solutions, freeze its optimal structure, and, for each new instance, optimize only the variational parameters. This eliminates structural search, cutting resolution time without loss of quality, and avoids any hardware reconfiguration, making the procedure immediately implementable on NISQ devices. \mathcal{A} thus becomes a reusable resource that significantly reduces TSP time-to-solution.

3 Proposed solution

Algorithm 1: Decoding permutation procedure

```

1 function PermutationDecoding( $\mathcal{P}$ ) is
2    $R \leftarrow [1, 2, \dots, n];$ 
3   for  $i \leftarrow n$  downto 1 do
4      $j \leftarrow 1 + (\mathcal{P} \bmod i);$ 
5      $\pi(n + 1 - i) \leftarrow R_j;$ 
6     remove  $R_j$  from  $R;$ 
7      $L \leftarrow \lfloor \mathcal{P}/i \rfloor;$ 
8   end
9   return  $\pi;$ 
10 end

```

The proposed method introduces two key innovations: the dynamic optimization of an \mathcal{A} tailored to a specific instance, and the reuse of the same optimized \mathcal{A} on previously unseen instances. Unlike most existing studies that rely on a fixed circuit topology, we co-optimize the \mathcal{A} layout itself to better suit the problem instance. This is accomplished through SA, which iteratively explores the space represented by rotation layer and entanglement patterns.

We decide to use an efficient encoding mechanism to represent our solution. As shown by [8], permutation encoding provides a more compact representation of a tour. Specifically, given a permutation π of n cities, we encode it as a single integer P_π in the range $[0, \dots, n! - 1]$. The original permutation can be recovered using the decoding procedure outlined in Algorithm 1, which requires only $\mathcal{O}(n)$ operations, making it highly scalable even for large n .

The approach we propose is summarized in Algorithm 2. It consists of two main components: (i) optimizing \mathcal{A} by calling SA with one of the TSP instances $t_0 \in \mathcal{T}$ (ii) “freezing” the best found solution’s structure and testing it on all remaining instances $\{\mathcal{T} \setminus t_0\}$. This procedure is inspired by the concept of *training* and *testing* phases from Machine Learning (ML). Similarly to ML, we *train* \mathcal{A} using a training set $\{t_0 \in \mathcal{T}\}$, and then *test* it using a testing set $\{\mathcal{T} \setminus t_0\}$.

Algorithm 2: Optimize, Freeze and Reuse

Data: set of TSP instances \mathcal{T}
Result: Optimized and Tested \mathcal{A} (with parameters)

- 1 generate random \mathcal{A} ;
- 2 use SA to optimize \mathcal{A} using $t_0 \in \mathcal{T}$ as benchmark;
- 3 freeze \mathcal{A} shape;
- 4 use \mathcal{A} to solve TSP problems in $\{\mathcal{T} \setminus t_0\}$

3.1 Ansatz Optimization

The first key component of our approach is utilizing the SA optimization algorithm to find the optimal \mathcal{A}_{best} for the TSP problem. We choose this method due to its capability of discovering an approximate global optimum in a large search space, avoiding local optima. Instead of employing a population-based approach, we opted for a single-individual algorithm as it can allocate all available resources towards fully exploring and refining one solution, thereby accelerating convergence and enabling more profound local search. Our SA implementation is detailed in Algorithm 3.

Selecting an appropriate \mathcal{A} size is challenging because excessively large circuits incur high computational costs, while undersized ones produce suboptimal results. To tackle this issue, we partition our \mathcal{A} into 5 distinct blocks, each of which can be either a *Rotation block* or an *Entanglement block*. Rotation blocks consist of rotation gates (R_x, R_y, R_z), whereas Entanglement blocks are constructed using CX gates (see [21]). The first block of \mathcal{A} is always a rotation block, followed by an entanglement block, and this alternating pattern continues until the final block, which is also a rotation block. Within each rotation block, every gate has an independent parameter $\Theta_i[j]$, where i denotes the block index and j represents the qubit index.

$$\begin{aligned} \mathcal{A} &= \langle R_{block}, CX_{block}, R_{block}, CX_{block}, R_{block} \rangle, \\ R_{block} &\in \{R_x, R_y, R_z\} \\ CX_{block} &\in \{\text{linear, reverse linear, full, circular, SCA}\} \end{aligned}$$

Let us take into account the following example:

$$\mathcal{A} = \langle R_z, \text{linear}, R_z, \text{reverse linear}, R_y \rangle \quad (1)$$

This \mathcal{A} is represented as a quantum circuit in Figure 1. The first block consists of R_z gates, one for each qubit, forming a rotation layer. This is followed by an entanglement block composed of linearly arranged CX gates. The pattern alternates between rotation and entanglement blocks, ending with a final rotation block of R_y gates.

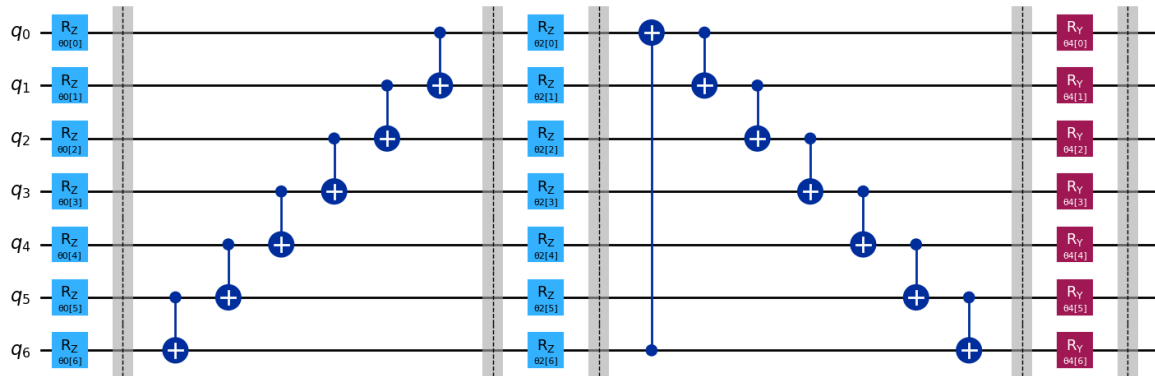


Figure 1: Quantum Circuit associated to example in (1)

The perturbations of $\mathcal{A}_{current}$, implemented by the **Perturbate** function (line 9), involve randomly selecting a block $b \in \mathcal{A}_{current}$ and replacing it with another distinct, valid block. This process modifies $\mathcal{A}_{current}$ to generate $\mathcal{A}_{neighbor}$ while ensuring compliance with the previously defined rules.

Algorithm 3: SA for Ansatz Optimization

Data: TSP instance $t_0 \in \mathcal{T}$
Result: Optimized \mathcal{A}_{best} (with parameters)

```
1  $T \leftarrow 1.0;$ 
2  $CoolingRate \leftarrow 0.999;$ 
3  $T_{min} \leftarrow 1 \times 10^{-3};$ 
4  $Iter_{max} \leftarrow 500;$ 
5  $iteration \leftarrow 0;$ 
6  $\mathcal{A}_{best} \leftarrow$  generate a random Ansatz;
7  $\mathcal{A}_{current} \leftarrow \mathcal{A}_{best};$ 
8 while  $T > T_{min}$  and  $iteration < Iter_{max}$  do
9    $\mathcal{A}_{neighbor} \leftarrow$  Perturbate( $\mathcal{A}_{current}$ );
10   $\Delta E \leftarrow$  Fitness( $\mathcal{A}_{neighbor}$ ) - Fitness( $\mathcal{A}_{current}$ );
11  if  $\Delta E > 0$  or RandomNumber()  $< e^{\frac{\Delta E}{T}}$  then
12     $\mathcal{A}_{current} \leftarrow \mathcal{A}_{neighbor};$ 
13    if Fitness( $\mathcal{A}_{current}$ )  $>$  Fitness( $\mathcal{A}_{best}$ ) then
14       $\mathcal{A}_{best} \leftarrow \mathcal{A}_{current};$ 
15    end
16  end
17   $T \leftarrow T \times CoolingRate;$ 
18   $iteration \leftarrow iteration + 1;$ 
19 end
```

The fitness value of a given \mathcal{A} is determined by executing its quantum circuit. The evaluation proceeds as follows:

1. **Initial Sampling:** We generate 100 random parameter vectors with angles in $[0, 2\pi]$ and compute their corresponding energy values.
2. **Selection:** The 10 vectors yielding the lowest energies are selected as initial points for optimization.
3. **Optimization:** Using the Powell algorithm [22], we refine these parameters to minimize the energy further.

The Powell algorithm was chosen after extensive comparisons with both gradient-based and gradient-free optimizers, as it demonstrated superior effectiveness and reliability in our experiments. After optimization, we execute the circuit n times using the refined parameters and record the outcomes. The fitness value is then computed as the empirical probability of observing the optimal permutation, defined as:

$$Fitness = \frac{\text{Number of optimal permutation observed}}{n} \quad (2)$$

This entire evaluation process is encapsulated in the **Fitness** procedure (Algorithm 4). The acceptance condition for replacing $\mathcal{A}_{current}$ with $\mathcal{A}_{neighbor}$ is implemented at line 11 of Algorithm 3 using the Metropolis criterion [23]. As a fundamental component of SA, this criterion enables an effective balance between: *exploration* of new solutions and *exploitation* of current solutions while maintaining the ability to escape local optima and progressively converge toward global optima in complex search spaces.

3.2 Reusing the Optimized Ansatz

Upon completion of the SA algorithm, we obtain the optimal \mathcal{A}_{best} and its associated parameters for the instance $t_0 \in \mathcal{T}$. The next step is to apply the freezing procedure: \mathcal{A} topology is fixed (no further structural changes are allowed) and it is used to solve all other instances in $\{\mathcal{T} \setminus t_0\}$. Our “freezing” procedure is listed in Algorithm 5.

Algorithm 4: Fitness computation

```
1 function Fitness( $\mathcal{A}$ ,  $T$ : int)  $\rightarrow$  float is
2   execute RunVQE( $\mathcal{A}$ )  $T$ -times and store the results;
3    $f \leftarrow$  compute the average value over stored results;
4   return  $f$ ;
5 end
6 function RunVQE( $\mathcal{A}$ )  $\rightarrow$  list[float] is
7    $S \leftarrow$  generate 100 random vector in range  $[0, 2\pi]$ ;
8   for  $s \in S$  do
9     | compute  $s$  energy;
10    end
11    $S_{start} \leftarrow$  find first 10 vectors with lowest energy;
12    $results \leftarrow$  empty list;
13   for  $n$  times do
14     |  $params \leftarrow$  Powell( $\mathcal{A}$ ,  $S_{start}$ );
15     | apply  $params$  to  $\mathcal{A}$ ;
16     |  $res \leftarrow$  execute VQE using  $\mathcal{A}$  ( $N = 1024$ );
17     |  $P_{opt} \leftarrow \frac{\text{number of correct solution found}}{N}$ ;
18     | add  $P_{opt}$  to  $results$ ;
19   end
20   return  $results$ ;
21 end
```

The core advantage of this approach lies in its ability to reuse a pre-optimized \mathcal{A} , both in structure and parameters, to solve new problem instances without restarting the full optimization process. The method simply requires local re-optimization via Powell's algorithm (line 3), using the previously identified optimal parameters from SA as starting points, to efficiently derive a new optimized parameter set specifically tailored to each target instance.

Algorithm 5: Freezing procedure

Data: \mathcal{A}_{best} , $OptParams_{\mathcal{A}_{best}}$, $\{\mathcal{T} \setminus t_0\}$
Result: P_{opt} foreach $t_i \in \{\mathcal{T} \setminus t_0\}$

```
1  $results \leftarrow$  empty list;
2 for  $t_i \in \{\mathcal{T} \setminus t_0\}$  do
3   |  $params \leftarrow$  Powell( $\mathcal{A}_{best}$ ,  $OptParams_{\mathcal{A}_{best}}$ );
4   | apply  $params$  to  $\mathcal{A}_{best}$ ;
5   |  $res \leftarrow$  execute VQE using  $\mathcal{A}_{best}$  ( $N = 1024$ );
6   |  $P_{opt} \leftarrow \frac{\text{number of correct solution found}}{N}$ ;
7   | add  $P_{opt}$  to  $results$ ;
8 end
```

4 Experiments

This section presents the experimental results of applying our VQA approach to the TSP.

4.1 Problem setup

We generate TSP instances using a controlled procedure, where each instance is represented by a symmetric $n \times n$ distance matrix, with n denoting the number of cities. Distances between cities are randomly sampled as integers within a predefined range (e.g., 1 to 100), while self-distances are set to 0 to ensure validity. This generation method enables the efficient construction of instances for testing and comparing algorithms across varying levels of complexity and problem size.

We generated 44 TSP instances in total, 11 for each city dimension (4,5,6,7). For each dimension, instance 0 is reserved for the training of \mathcal{A} , while instances 1 – 10 form the test set used to evaluate the generalization of the algorithm.

This configuration also allows the optimal tour cost to be calculated through an exhaustive enumeration of all city permutations by a classical method, providing an exact reference solution. This exact value serves as a benchmark to assess the performance of our VQA approach, by comparing the cost of the generated tours against the known optimum. The number of qubits and \mathcal{A} parameters required for each instance size is reported in Table 1.

Table 1: Qubit and Ansatz parameter count required for different city sizes.

City nodes	Qubits used	Ansatz parameters
4	5	15
5	7	21
6	10	30
7	13	39

4.2 Experimental Setup

We implemented the Algorithm 3 in Python using the Qiskit library [21]. For each problem size, we ran 5 independent executions of the VQA and evaluated the mean tour length returned by the best-found circuit, using 1024 measurement shots to ensure statistical robustness. We also archived all observed tour lengths, allowing for a direct assessment of the circuit’s ability to produce the exact optimal tour, which was previously determined through exhaustive enumeration of all permutations.

As a classical baseline, we implemented a SA heuristic capped at 500 iterations. The search commenced at a temperature T of 1.0 and followed a cooling rate that multiplied the temperature by 0.999 at each step, terminating when the temperature dropped below 0.001 or the iteration limit was reached.

4.3 Results

In this section we describe in detail the results with respect to the experimental method adopted to evaluate the effectiveness of our VQA on the TSP problem.

The goal is to demonstrate how the proposed method behaves as the problem size varies (4 to 7 cities) and to quantify the probability of finding the optimal solution.

4.3.1 Convergence to the optimal solution

To evaluate the convergence of our Ansatz optimization method, in this section we focus on a single training instance. The goal is not to compare all 10 problem settings, but rather to illustrate the behavior of the algorithm during training and to highlight the effectiveness of our parameter tuning and \mathcal{A} strategy. This focused analysis demonstrates the efficiency with which the proposed optimization scheme drives the circuit toward high-quality solutions.

The trend of *fitness* that we see in Figure 2 confirms that the algorithm, thanks to the optimized \mathcal{A} , quickly reaches a near-optimal tour and then takes a modest number of steps to fix its optimality. This result demonstrates the efficiency of the adopted optimization process.

Best Ansatz found Figure 3 shows the variational circuit that, after the optimization phase, provided the lowest tour value for the training instance with 5 cities. The architecture employs all 7 available qubits and is divided into 3 parametric blocks separated by barriers highlighting the logical structure.

The optimal \mathcal{A} follows a simple but effective scheme:

$$\begin{aligned}
 \text{R}_z \text{ layer} &\longrightarrow \text{full entanglement} \longrightarrow \text{R}_z \text{ layer} \\
 &\longrightarrow \text{linear entanglement} \longrightarrow \text{R}_z \text{ layer}.
 \end{aligned}$$

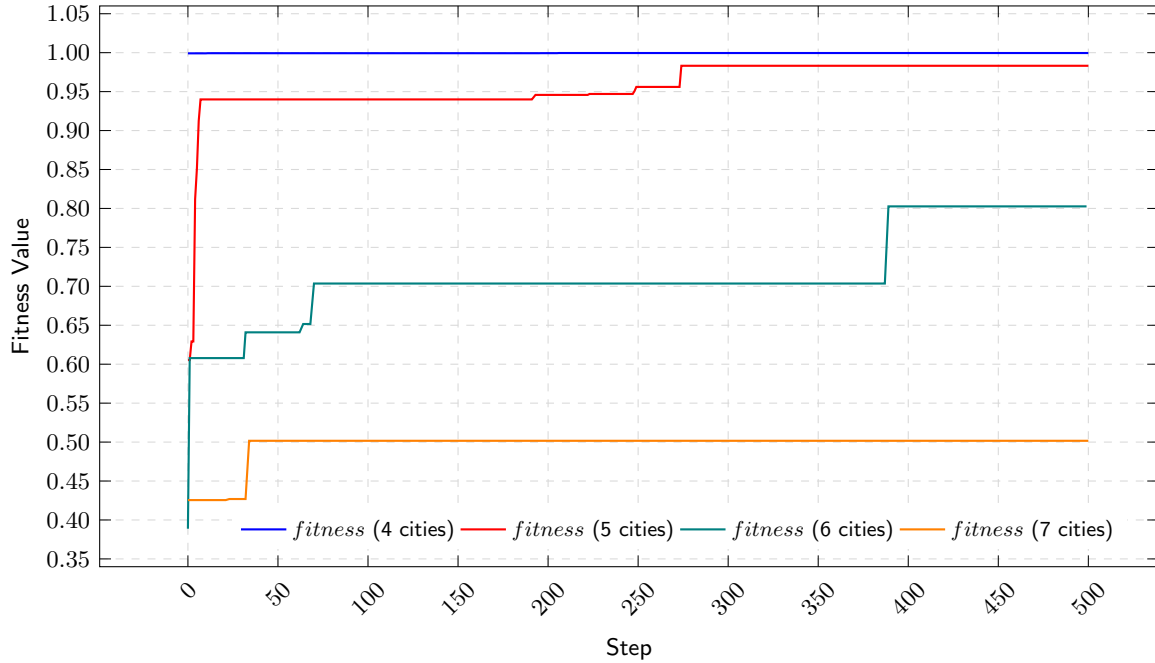


Figure 2: Convergence of SA toward the optimal solution probability for TSP instances with 4, 5, 6 and 7 cities (index 0, training set). The fitness evolves by 500 steps.

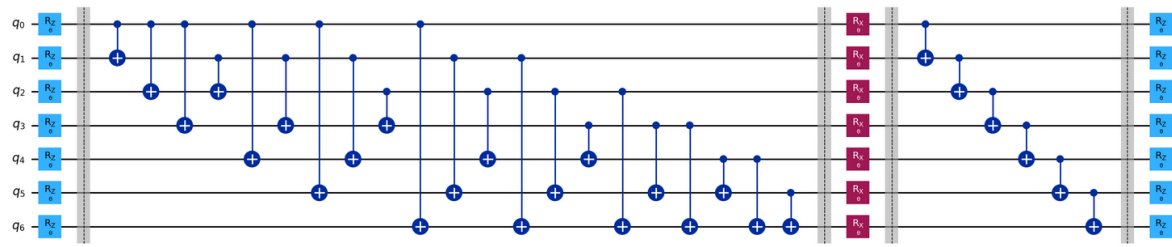


Figure 3: Best Ansatz found for training instance with 5 nodes

Concretely, each qubit is first rotated around the z axis (R_z). These single qubit phases are then mixed by a fully connected CX block, which connects each qubit with all others. A second layer of R_x refines the phases introduced so far, after which a CX scheme provides linear entanglement. The circuit closes with the R_z layer.

4.3.2 Reusing

In this section we apply the optimization structure to unseen problem, and evaluate the performance of the \mathcal{A}_{best} training. The table 2 reports, for each problem dimension, how many of the 10 test TSP instances achieve an optimal tour sampling probability above a prescribed τ success threshold. In the four-city benchmark, the \mathcal{A} generalizes perfectly: all instances meet even the most stringent requirement, $\tau = 0.90$, leading to a success rate of 100%. When the search space grows to five cities, the circuit remains highly reliable: 9 of the 10 instances pass each threshold up to $\tau = 0.80$, while one instance fails to meet the more restrictive 90% threshold. This shows that even a modest increase in combinatorial complexity can bring up occasional, but significant, generalization difficulties. The six-city benchmark highlights the emergence of scalability limitations: with a relatively permissive threshold ($\tau \leq 0.60$), the circuit still solves six of the ten instances, while imposing more stringent requirements ($\tau = 0.80$ or 0.90) reduces the number of successes to four. This result indicates that, although some six-city instances exceed the circuit's capacity, a significant portion continue to be successfully solved, signaling good generalization in many cases.

The deterioration becomes evident as it grows to seven cities. As Tab. 2 shows, with a very

permissive success threshold, $\tau = 0.20$, the algorithm manages to sample the optimal tour in only 3 of the 10 test instances. Increasing the threshold to $\tau = 0.40$ reduces the successes to 2, and the count remains stuck at 2 for all subsequent thresholds. In other words, in 80% times of the seven-city instances the probability of extracting the optimum remains below 0.60%, and in 60% of the cases it never exceeds 0.20%. This sharp decline confirms that the current method does not efficiently generalize the larger search space created.

Table 2: For each threshold τ , number of test cases ($n_{inst} = 10$) in which the optimal tour probability satisfies $P_{opt} \geq \tau$.

Threshold τ	#Instances with $P_{opt} \geq \tau$			
	4 Cities	5 Cities	6 Cities	7 Cities
0.20	10	9	6	3
0.40	10	9	6	2
0.60	10	9	6	2
0.80	10	9	4	2
0.90	10	8	4	2

Therefore, reuse of the \mathcal{A} , accompanied by re-optimization of previously learned parameters, ensures uniform excellence in four-city problems, high but not perfect robustness in five-city problems, and highly instance-dependent performance in six-city problems. This behavior provides a clear quantitative benchmark for identifying instances where better performing circuits or different optimization strategies will be needed to maintain high performance.

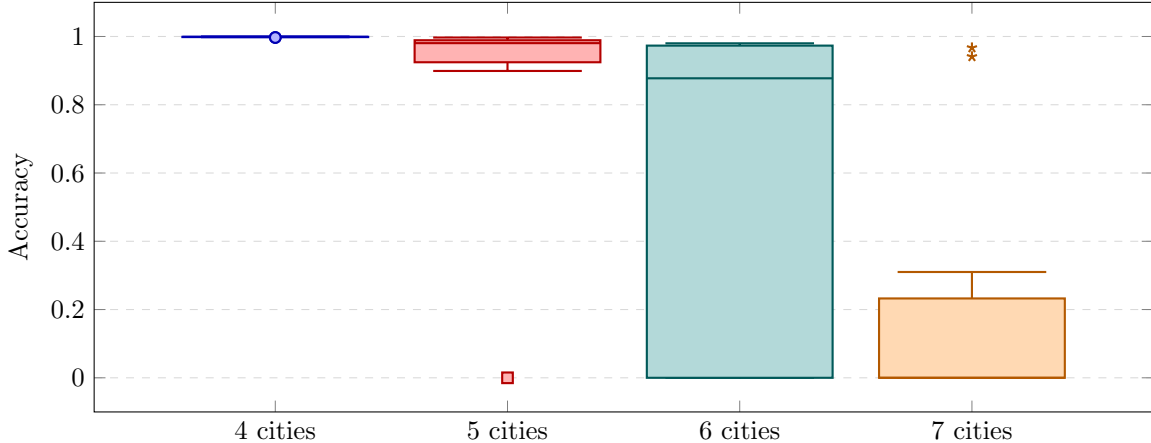


Figure 4: Distribution of solution accuracy across the four problem-size (city-count) scenarios.

In Figure 4 we see that, for instances with 4 cities, the algorithm always returns the optimal tour. All runs coincide with an accuracy of 1.0, producing zero variance; the distribution shows that the median, quartiles and extremes are identical.

For the 5-city instances (red box), the distribution remains narrow and is centered just below 1.0. The inter-quartile range (IQR), i.e., the distance between the third and first quartiles, $Q_3 - Q_1$ [28], extends by a few percentage points, showing that almost every run reaches the optimal or near-optimal tour. A single outlier at 0, however, reveals that the algorithm converges to a completely wrong minimum.

In contrast, the 6 city instances (green box) show this graph: the lowest 25% of runs collapse near 0, while the highest 25% exceeds 0.9. Although the median remains high (about 0.9), the large IQR (about 0.9) indicates that performance is highly dependent on instance and initialization, oscillating between perfect and completely wrong solutions.

For the most challenging instances at 7 city (orange box in Fig. 4) performance plummets. The median accuracy drops to ≈ 0.20 , with first quartile $Q_1 \approx 0.02$ and third quartile $Q_3 \approx 0.25$, so that the inter-quartile range holds of 0.23%. Both “whiskers” remain anchored at the low end of the axis

(whisker lower than 0, upper 0.25) and only two high outliers appear, around ≈ 0.90 . In probabilistic terms, this implies that at least 75% of the runs sample the optimal tour with probability less than 0.25, indicating that the generalization ability of the circuit deteriorates almost completely when the problem size reaches seven cities.

5 Conclusions and Future Work

This paper introduces an optimization-freezing-reuse study to address TSP with variational algorithms. By a compact encoding of permutations, the qubit mapping drops to $\mathcal{O}(n \log n)$, making the representation of TSP instances much more efficient.

Searching with SA for the optimal \mathcal{A} , mutating the circuit topologies and accepting changes according to the Metropolis criterion, produces after a hundred iterations a shallow but performant architecture for solving the problem.

Once the structure is “frozen”, a slight re-optimization of the parameters by Powell alone sustains impressive performance on unseen instances, with perfect accuracy for 4 city problems, 90% for 5 cities, and an average accuracy of 80% for six cities; and, although declining markedly, an average accuracy of about 20% for 7 cities, with rare outliers close to 0.9%, sign that already at this scale the \mathcal{A} shows its limitations.

The big advantage of this method is that, by skipping the costly structural research in testing, execution times collapse, making the approach immediately testable on current NISQ devices. However, the very performance collapse observed at 7 cities indicates that progress is needed on both the algorithmic and hardware fronts.

The next steps are clear. It will be critical to put it to the test on real quantum hardware, such as superconducting or ion trap-based hardware. In this context, it will be imperative to adopt error mitigation techniques, which are essential to separate the intrinsic performance of the algorithm from the effects of decoherence and noise to identify the real bottlenecks of the proposed method on real hardware.

From an algorithmic point of view, a natural evolution is to replace the Powell-based training or testing phase with methods that make use of the gradient, such as Adam or SPSA. These optimizers could not only speed up convergence, but also maintain or even improve accuracy as the problem size grows. In parallel, initializing circuit parameters with warm-start strategies derived from classical heuristics would allow starting from configurations already close to good-quality solutions, significantly reducing the training cost as the number of cities increases.

Finally, it would be extremely interesting to apply the optimize-freeze-reuse paradigm to even more complex permutation problems, such as the Vehicle Routing Problem (VRP) and Job-Shop Scheduling (JSS). Both share the burden of exploring an endless combinatorial space, but introduce additional constraints that can be handled with penalty terms or, integrated directly into the \mathcal{A} . Demonstrating the robustness of the method on VRP and JSS would not only prove the usefulness and operation of the method, but also pave the way for the application of the workflow to a whole class of NP-hard problems of great industrial relevance.

References

- [1] A. Peruzzo, J. McClean, P. Shadbolt, M. H. Yung, X. Zhou, P. Love, A. Aspuru-Guzik, and J. O’Brien, “A variational eigenvalue solver on a quantum processor,” *Nature communications*, vol. 5, 2013.
- [2] A. Kandala, A. Mezzacapo, K. Temme, M. Takita, M. Brink, J. M. Chow, and J. M. Gambetta, “Hardware-efficient variational quantum eigensolver for small molecules and quantum magnets,” *Nature*, vol. 549, no. 7671, pp. 242–246, 2017.
- [3] M. Cerezo, A. Arrasmith, R. Babbush, S. C. Benjamin, S. Endo, K. Fujii, J. R. McClean, K. Mitarai, X. Yuan, L. Cincio, and P. J. Coles, “Variational quantum algorithms,” *Nature Reviews Physics*, vol. 3, no. 9, pp. 625–644, 2021.
- [4] J. Preskill, “Quantum computing in the NISQ era and beyond,” *Quantum*, vol. 2, p. 79, 2018.

- [5] K. Bharti, A. Cervera-Lierta, T. H. Kyaw, T. Haug, S. Alperin-Lea, A. Anand, M. Degroote, H. Heimonen, J. S. Kottmann, T. Menke, W.-K. Mok, S. Sim, L.-C. Kwek, and A. Aspuru-Guzik, “Noisy intermediate-scale quantum algorithms,” *Reviews of Modern Physics*, vol. 94, no. 1, p. 015004, 2022.
- [6] E. Farhi, J. Goldstone, and S. Gutmann, “A quantum approximate optimization algorithm,” *arXiv preprint arXiv:1411.4028*, 2014.
- [7] T. Albash and D. A. Lidar, “Adiabatic quantum computation,” *Reviews of Modern Physics*, vol. 90, no. 1, p. 015002, 2018.
- [8] M. Schnaus, L. Palackal, B. Poggel, X. Runge, H. Ehm, J. M. Lorenz, and C. B. Mendl, “Efficient encodings of the travelling salesperson problem for variational quantum algorithms,” in *2024 IEEE International Conference on Quantum Software (QSW)*, pp. 81–87, July 2024.
- [9] D. L. Applegate, R. E. Bixby, V. Chvátal, and W. J. Cook, *The Traveling Salesman Problem: A Computational Study*. Princeton University Press, 2006.
- [10] M. Dorigo and L. M. Gambardella, “Ant colonies for the travelling salesman problem,” *BioSystems*, vol. 43, no. 2, pp. 73–81, 1997.
- [11] D. E. Goldberg and R. Lingle, “Alleles, loci, and the traveling salesman problem,” in *Proceedings of the First International Conference on Genetic Algorithms*, pp. 154–159, 1985.
- [12] E. Hickman, A. Roth, and Y. Zhu, “Comparison of unitary coupled cluster ansatz methods for the variational quantum eigensolver,” 2019.
- [13] V. Padmasola, Z. Li, R. Chatterjee, and W. Dyk, “Solving the traveling salesman problem via different quantum computing architectures,” *arXiv preprint arXiv:2502.17725*, 2025.
- [14] M. Alawir, M. A. Alatasi, H. Salloum, and M. Mazzara, “Enhanced quantum annealing tsp solver (EQATS): Advancements in solving the traveling salesman problem using D-Wave’s quantum annealer,” in *Proc. 2024 IEEE Int. Conf. on Quantum Software*, Dec. 2024.
- [15] S. Jain, “Solving the traveling salesman problem on the D-Wave quantum computer,” *Frontiers in Physics*, vol. 9, 2021.
- [16] Y. Ruan, S. Marsh, X. Xue, Z. Liu, and J. Wang, “The quantum approximate algorithm for solving traveling salesman problem,” *Computers, Materials & Continua*, vol. 63, no. 3, pp. 1237–1247, 2020.
- [17] W. Qian, R. A. M. Basili, M. M. Eshaghian-Wilner, A. Khokhar, G. Luecke, and J. P. Vary, “Comparative study of variations in quantum approximate optimization algorithms for the traveling salesman problem,” *Entropy*, vol. 25, no. 8, p. 1238, 2023.
- [18] M. Shi, S. Wu, Y. Li, G. Yuan, C. Yao, and G. Chen, “A quantum framework for combinatorial optimization problem over graphs,” *Data Science and Engineering*, vol. 10, no. 2, pp. 246–257, 2025.
- [19] D. Bertsimas and J. Tsitsiklis, “Simulated annealing,” *Statistical Science*, vol. 8, no. 1, pp. 10–15, 1993.
- [20] A. Javadi-Abhari, M. Treinish, K. Krsulich, C. J. Wood, J. Lishman, J. Gacon, S. Martiel, P. D. Nation, L. S. Bishop, A. W. Cross, B. R. Johnson, and J. M. Gambetta, “TwoLocal,” *Qiskit API documentation*, 2024.
- [21] A. Javadi-Abhari, M. Treinish, K. Krsulich, C. J. Wood, J. Lishman, J. Gacon, S. Martiel, P. D. Nation, L. S. Bishop, A. W. Cross, B. R. Johnson, and J. M. Gambetta, “Quantum computing with Qiskit,” *arXiv preprint arXiv:2405.08810*, 2024.
- [22] M. J. D. Powell, “An efficient method for finding the minimum of a function of several variables without calculating derivatives,” *The Computer Journal*, vol. 7, no. 2, pp. 155–162, 1964.

- [23] N. Metropolis, A. W. Rosenbluth, M. N. Rosenbluth, A. H. Teller, and E. Teller, “Equation of state calculations by fast computing machines,” *The Journal of Chemical Physics*, vol. 21, no. 6, pp. 1087–1092, 1953.
- [24] M. Jünger, G. Reinelt, and G. Rinaldi, “The traveling salesman problem,” in *Handbooks in Operations Research and Management Science*, vol. 7, pp. 225–330, Elsevier, 1995.
- [25] D. J. Egger, J. Mareček, and S. Woerner, “Warm-starting quantum optimization,” *Quantum*, vol. 5, p. 479, 2021.
- [26] J. A. Montañez-Barrera, D. Willsch, and K. Michelsen, “Transfer learning of optimal QAOA parameters in combinatorial optimization,” *Quantum Information Processing*, vol. 24, no. 5, 2025.
- [27] A. Cervera-Lierta, J. S. Kottmann, and A. Aspuru-Guzik, “Meta-variational quantum eigensolver: Learning energy profiles of parameterized hamiltonians for quantum simulation,” *PRX Quantum*, vol. 2, no. 2, 2021.
- [28] J. W. Tukey, *Exploratory Data Analysis*. Addison-Wesley, Reading, MA, 1977.